Immortalization and functional screening of natively paired human T cell receptor repertoires

Ahmed S. Fahad 1,†, Cheng-Yu Chung1,†, Sheila N. Lopez Acevedo1, Nicoleen Boyle1, Bharat Madan1, Matias F. Gutiérrez-González1, Rodrigo Matus-Nicodemos2, Amy D. Laflin1, Rukmini R. Ladi1, John Zhou1, Jacy Wolfe1, Sian Llewellyn-Lacey3, Richard A. Koup2, Daniel C. Douek2, Henry H. Balfour Jr4,5, David A. Price3,6 and Brandon J. DeKosky 1,7,8,9,*

1Department of Pharmaceutical Chemistry, The University of Kansas, Lawrence, KS 66044, USA
2Vaccine Research Center, National Institute of Allergy and Infectious Diseases, National Institutes of Health, Bethesda, MD 20892, USA
3Division of Infection and Immunity, Cardiff University School of Medicine, University Hospital of Wales, Cardiff CF14 4XN, UK
4Department of Laboratory Medicine and Pathology, University of Minnesota Medical School, Minneapolis, MN 55455, USA
5Department of Pediatrics, University of Minnesota Medical School, Minneapolis, MN 55455, USA
6Systems Immunity Research Institute, Cardiff University School of Medicine, University Hospital of Wales, Cardiff CF14 4XN, UK
7Department of Chemical Engineering, The University of Kansas, Lawrence, KS 66044, USA
8Department of Chemical Engineering, Massachusetts Institute of Technology, Cambridge, MA 02142, USA
9 The Ragon Institute of MGH, MIT, and Harvard, Cambridge, MA 02139, USA

*To whom correspondence should be addressed. E-mail: dekosky@mit.edu †These authors contributed equally. Abstract Functional analyses of the T cell receptor (TCR) landscape can reveal critical information about protection from disease and molecular responses to vaccines. However, it has proven difficult to combine advanced next-generation sequencing technologies with methods to decode the peptidemajor histocompatibility complex (pMHC) specificity of individual TCRs. We developed a new high-throughput approach to enable repertoirescale functional evaluations of natively paired TCRs. In particular, we leveraged the immortalized nature of physically linked TCRα:β amplicon libraries to analyze binding against multiple recombinant pMHCs on a repertoire scale, and to exemplify the utility of this approach, we also performed affinity-based functional mapping in conjunction with quantitative next-generation sequencing to track antigen-specific TCRs. These data successfully validated a new immortalization and screening platform to facilitate detailed molecular analyses of disease-relevant antigen interactions with human TCRs.

Keywords: T cell receptor (TCR), high-throughput TCRα:β sequencing, library immortalization, affinity-based screening

Introduction T cells form an essential component of adaptive immunity. Each human possesses billions of T cells, each of which expresses a somatically rearranged heterodimeric T cell receptor (TCR). In turn, each TCR recognizes a unique array of peptides bound to cell surface–expressed peptide-major histocompatibility complex (pMHC) molecules (Krogsgaard and Davis, 2005). A detailed molecular understanding of CD4+ and CD8+ T cell responses is critically important for continued progress in human immunology and the rational development of immune-based therapies and vaccines. However, this goal is complicated by the fact that each individual expresses up to six different MHC class I proteins (two allotypes each for HLAA, HLA-B and HLA-C) and up to six different MHC class II proteins (two allotypes each for HLA-DP, HLA-DQ and HLA-DR), all of which bind distinct

subsets of the universal peptidome, and by the size of the TCR specificity landscape, which has been estimated to exceed a theoretical diversity of 1015 (ref Sewell, 2012).

It is currently impossible to analyze all potential interactions that could occur in any given individual between pMHC molecules and TCRs. Most technologies to identify and monitor antigen-specific TCR sequences rely on screening limited numbers of viable T cells in blood or tissue samples. Moreover, the composition of T cell libraries can be altered by repeated in vitro expansion, which is necessary for studies of antigen specificity (Koning et al., 2014), and methods based on limiting dilution or the isolation of single cells are generally restricted to small-scale analyses of TCRα:β pairs (Linnemann et al., 2013; Yossef et al., 2018; Hu et al., 2018; Scheper et al., 2019). The difficulties associated with maintaining and studying primary human T cells in vitro have also prevented functional screening against large panels of different pMHC antigens. In addition, fate decisions and functional responses are largely dictated by TCR affinity in the context of any given pMHC, and accordingly, technologies that enable the quantification of TCR affinity across multiple pMHCs are highly desirable (Aleksic et al., 2010; King et al., 2012; Vazquez-Lombardi et al., 2020).

Several new approaches to high-throughput TCR analysis have emerged in recent years. Impressive efforts have leveraged the power of single-cell transcriptomics to identify increasing numbers of antigen-specific clonotypes, but these studies are still limited by the labile nature of primary human T cells and the inability to perform repeated functional interrogations against TCR libraries (Szabo et al., 2019; Corridoni et al., 2020; Zhang et al., 2021). Improved high-throughput technologies are therefore needed to characterize the scope of TCR interactions against pMHC antigens. Mass cytometry enables screening against large panels of metal-conjugated pMHCs but fails to capture functional connections with individual TCR sequences (Ornatsky et al., 2006; Newell and Davis, 2014; Strønen et al., 2016; Glanville et al., 2017). Prior efforts have also analyzed T cell binding to multiple specificities using DNA barcoded pMHCs, but single-cell binding information is still generally limited to relatively small numbers of TCR clones (Bentzen et al., 2016; Zhang et al., 2018; Overall et al., 2020; Ma et al., 2021; Nesterenko et al., 2021; Minervina et al., 2021). Singlecell transcriptome sequencing has emerged as one prevalent platform for TCRα:β discovery (Azizi et al., 2018; Zhang et al., 2020; Gantner et al., 2020; Nesterenko et al., 2021). However, these droplet-based methods are incompatible with large-scale TCRα:β gene immortalization, which precludes renewable functional screening and high-throughput affinity assays against broad pMHC panels.

High-throughput functional screening is critical for the identification of antigen cross-reactivity mediated by degenerate TCRs. Cross-reactivity has been associated with enhanced immune protection against variable pathogens (Grant et al., 2018; Mendoza et al., 2020; Mateus et al., 2020), but crossreactivity can also lead to adverse patient outcomes in the context of immunotherapeutic TCRs (Linette et al., 2013). Natively paired TCRα:β chains have been recovered from single cells and expressed in reporter cell lines to analyze functional reactivity (Guo et al., 2016; Hu et al., 2018; Spindler et al., 2020; Nesterenko et al., 2021). However, these approaches are limited in scope, and library-scale methods that enable affinity-based screening are urgently needed to fully characterize the repertoire of antigen-specific TCRs.

To address these challenges, we developed a new approach based on the renewable nature of T cell libraries to screen for antigen-specific TCRs, exemplified in the context of patients with acute infectious mononucleosis (IM). Our method links natively paired TCRα:β gene sequences with their cognate pMHC targets. In addition, we measured the compound interaction affinities of individual TCRs, providing critical information on functional recognition needed to measure crossreactivity in large pMHC panels. This new molecular platform will enable comprehensive functional studies of

human T cell immunity in health and disease and accelerate the discovery of safe and effective immunotherapies based on TCRs.

Results

Single-cell cloning and sequencing of natively paired TCRα:β libraries We previously described an emulsion-based technology for single-cell analysis of natively paired antibody heavy and light chains (DeKosky et al., 2015, 2016; McDaniel et al., 2016; Lagerman et al., 2019), integrated with a cloning approach that allowed functional expression and screening of physically linked antibody heavy:light cDNAs (Wang et al., 2018; Fahad et al., 2021; Banach et al., 2021). Here, we modified these immune receptor display technologies to implement highthroughput screening and functional expression of natively paired TCRα:β sequences obtained from >106 individual T cells per sample. T cells were obtained from peripheral blood mononuclear cells (PBMCs) of three acute infectious mononucleosis patients with acute IM (Fig. 1, Supplementary Table SI) (Balfour et al., 2013; Grimm et al., 2016). A flow-focusing emulsification system was used to encapsulate single cells inside droplets containing poly-dT-coated magnetic beads to capture polyadenylated mRNAs. The magnetic beads were recovered, re-emulsified and subjected to an overlap extension RT-PCR reaction physically linked TCRα and TCRβ amplicons onto the same cDNA strand (Supplementary Fig. S1a, Supplementary Table SII, see Materials and Methods) (DeKosky et al., 2013, 2015; McDaniel et al., 2016). cDNA amplicons were analyzed by next-generation sequencing (NGS), and a nested PCR reaction was performed to generate TCRα:β amplicons for cloning into a new lentiviral expression vector, enabling library-scale display of the natively paired TCRα:β genes (Fig. 1 and Supplementary Fig. S1b).

All three patients were seropositive for Epstein–Barr virus (EBV) at the time of sample acquisition (Supplementary Table SI). We began with an average of 10 × 106 primary PBMCs from each patient, and following a brief period of in vitro stimulation, we analyzed TCRα:β amplicons via NGS and cloned the corresponding expression libraries into J.RT3-T3.5/CD8 cells (Fig. 1a-c and Supplementary Tables SII–SIII). Initial NGS analysis revealed 7,315,096 natively paired TCRα:β sequences. The data were then filtered for quality, clustered according to TCRβ chain nucleotide identity and parsed to eliminate paired TCRα:β sequences with a read count of 1, leaving a total of 42,143 unique TCRα:β quality-filtered clusters across all three patients. Diverse TCR gene usage was observed in each library, confirming that large numbers of TCRs were recovered from each donor (Fig. 2a, Supplementary Table SIII). Donor 1 T cells were expanded in vitro and divided into two biological replicates for Vα:Vβ sequence analysis (see Materials and Methods). We observed a high proportion of overlapping unique CDRβ3 clusters in the two Donor 1 replicates as measured by exact CDR-β3 amino acid match (3753 overlapping CDR-β3 clusters out of 7284 clusters with a read count ≥2 in Replicate 1, representing an overlap of 51.5%). As expected, small numbers of TCRβ sequences were shared among the repertoires across different donors (Fig. 2b), each validated with a read count ≥2 to minimize the inclusion of amplification and sequencing errors in the final dataset (DeKosky et al., 2016; McDaniel et al., 2016; Wang et al., 2018; Lagerman et al., 2019; Fahad et al., 2021). Other recent studies included single-read TCRα:β sequences for repertoire-scale bioinformatic analyses (Spindler et al., 2020), and the corresponding analyses of our data are reported in the supplement to enable direct comparisons with prior reports (Supplementary Table SIII).

Screening natively paired TCRα:β libraries against pMHC tetramers We cloned TCRα:β amplicons into an immortalized surface display platform to enable library-scale interrogation of TCR binding to soluble pMHC antigens via fluorescence-activated cell sorting (FACS). Immortalized TCR libraries were screened using fluorescent pMHC tetramers, recovered via FACS an analyzed by NGS to identify antigen-specific TCRs (Fig. 1d-e, Supplementary Fig. S1b).

Paired TCRα:β amplicons were cloned into a lentiviral vector display system using an approach modified from previous studies (Wang et al., 2018; Fahad et al., 2021; Banach et al., 2021). The vector contained a leader sequence for TCRβ expression at one end of the restriction enzyme cut sites, with the required components of the TCRα constant region at the other end of the cut sites. We also included an internal ribosomal entry site (IRES) and an mCherry marker to identify TCRα:β expression via FACS (Supplementary Fig. S1b). After cloning the TCRα:β amplicons, the linker region was swapped with a linear construct containing the remaining portion of the TCRβ constant region, a sequence derived from porcine teschovirus-1 (P2A) (Liu et al., 2017), and a leader sequence for TCRα expression (Supplementary Fig. S1b). At least 106 transformants were maintained at each cloning step to preserve TCRα:β diversity (Wang et al., 2018; Fahad et al., 2021; Banach et al., 2021). The expression plasmids were packed into lentiviral particles for transduction into J.RT3- T3.5/CD8 cells, generating immortalized TCRα:β surface display libraries with the potential for limitless propagation. We then leveraged the renewable nature of J.RT3-T3.5/CD 8 cell libraries to screen the expressed TCRα:β repertoires against multiple pMHCs. Each library was sorted for mCherry expression via FACS. mCherry+ TCRα:β-J.RT3-T3.5/CD8 libraries were then expanded and stained with a panel of EBVderived pMHC antigens matched to the genetic background of each donor, using well-characterized fluorescent pMHC tetramers (Supplementary Table SIV). In line with the diagnosis of acute IM, substantial reactivity was observed against EBV (Fig. 3). Cells labeled with fluorescent pMHC tetramers were collected, cultured and sorted again to enrich the libraries for antigen-specific TCRs (Fig. 3, Supplementary Fig. S2). After two rounds of expansion, sorted cells were enriched 10- to 100-fold compared to the mCherry+ TCRα:βJ.RT3-T3.5/CD8 libraries (Fig. 3, Supplementary Fig. S2).

Identification of library-expressed TCRs specific for EBV

Expression libraries were sampled across each round of expansion and analyzed via NGS to quantify and track antigen-specific TCRs. We first picked single plasmid colonies after TCRα:β- J.RT3-T3.5/CD8 library amplification to validate our methodology. Single-colony analyses yielded seven unique clonotypes that bound to the TLD/HLAA∗02:01, QAK/HLA-B∗08:01 or RAK/HLA-B∗08:01 epitopes derived from EBV (Table I, Supplementary Table SIV). The specificities of these clonotypes were maintained after expression as monoclonal TCRs (Fig. 4a). We then analyzed the paired TCRα:β sequences in each library via NGS. Using this approach, we identified and validated an additional four EBV-specific TCRα:β clonotypes that had been enriched > 30-fold after the final round of expansion. In particular, Clone 6 and Clone 8 bound to QAK/HLAB∗08:01, whereas Clone 7 and Clone 11 bound to RAK/HLAB∗08:01 (Figs 4a and 5b, Supplementary Table SIV). Of note, Clone 7 expressed a previously identified public TCRβ chain (Miconnet et al., 2011; Koning et al., 2013, 2014), providing additional independent confirmation of TCR specificity. Functional validation of EBV-specific TCRs To validate functional specificity of these clonotypes, we transduced the corresponding TCRα:β lentiviral particles into SKW-3 cells. These reporter lines were then exposed to antigen-presenting cells (APCs) expressing donor-matched HLA molecules pulsed with the relevant peptide. The transformed SKW-3 cells were analyzed for surface expression of CD69, a common activation marker, and CD3, demarcating expression of the TCR (Nguyen et al., 2014; Mayassi et al., 2019). As expected, TCR-SKW-3 clones upregulated CD69 and downregulated CD3 after exposure to cognate pMHCs and, importantly, remained quiescent after exposure to noncognate pMHCs (Fig. 4b, Supplementary Fig. S3). Overall, we found that 11/11 (100%) of the tested monoclonal TCRs that bound a cognate tetramer in the J.RT3- T3.5/CD8 cell display system also induced cellular activation in SKW-3 cells exposed to the corresponding pMHC.

Bulk techniques for assessing avidity of antigen-specific TCRs

TCR avidity is a translationally relevant parameter that identifies clonotypes with the capacity to recognize low densities of surface-expressed pMHCs. To evaluate such measurements in the context of our system, we stained the Donor 3 library with three different concentrations of the RAK/HLA-B∗08:01 tetramer, ranging from 1 μg/mL down to 0.0039 μg/mL (Fig. 5a). Titration-based affinity assays fractionate the libraries based on differences in binding at various concentrations (Fig. 5a) and are commonly used to assess library-scale interactions (Harris et al., 2016; Starr et al., 2020). Clear separation of the library into two distinct cell populations was observed at a tetramer concentration of 0.0625 μg/mL (Fig. 5a, middle plot), whereas only one cell population was observed at a tetramer concentration of 0.0039 μg/mL (Fig. 5a, right plot). Sequence analysis of these avidity-defined cell populations revealed the presence of two distinct monoclonal TCRs. Clone 10 was highly enriched in sort gate J (95%), indicating a low avidity for RAK/HLAB∗08:01, whereas Clone 11 was highly enriched in sort gate I (75.7%) and in the cell population identified at a tetramer concentration of 0.0039 μg/mL (77%), indicating a high avidity for RAK/HLA-B∗08:01. The ability of our platform to support library-scale avidity measurements was further confirmed by expressing the sequences derived from Clone 10 and Clone 11 as monoclonal TCRs (Fig. 5b, Supplementary Fig. S4). These data confirmed that library-scale TCRα:β screening based on soluble pMHC titrations can compare the avidities of antigen-specific TCRs using bulk library-scale approaches paired with quantitative NGS data analysis.

Discussion

Library-scale functional characterization of human TCRα:β specificity is a technically demanding task that is nonetheless critical for the advancement of clinical biotechnologies and for our understanding of human immunology. We developed and validated a new approach to this challenge based on TCR repertoire immortalization, iterative library screening against panels of pMHCs and the functional characterization of monoclonal TCRs. Our platform was adapted from previously reported strategies designed to link the functional and genetic features of natively paired antibody repertoires (Wang et al., 2018; Fahad et al., 2021; Banach et al., 2021; Madan et al., 2021), enabling a greater analytical throughput compared with previous single-cell studies of natively paired TCRs (Trautmann et al., 2005; Day et al., 2007; Linnemann et al., 2013; Nesterenko et al., 2021). Of note, one microfluidic study demonstrated an ability to capture diverse clonotypes using a related approach and implemented two screening strategies to reduce the false-positive and false-negative discovery rates (Spindler et al., 2020). Here we identified an average of 14 047 unique TCRα:β sequences per sample, excluding singletons, which we believe are less reliable than clonotypes with ≥2 exact nucleotide-matched reads in datasets generated using NGS. Our data compared favorably with other highthroughput approaches incorporating functional analyses of TCRs (Spindler et al., 2020; Zhang et al., 2021), and additional improvements in library efficiency and yield will be gained as the technology matures.

The ability to mine affinity-specificity relationships is clearly important for the rational design and discovery of protective TCRs (Schmid et al., 2010; Campillo-Davo et al., 2020). Rapid affinity-based isolation procedures could also expedite the delivery of autologous immunotherapies with minimal off-target effects to enhance drug efficacy and provide an inherent degree of safety. Our platform recovered individual antigen-specific TCR clonotypes with initial library frequencies as low as 0.00001, which were substantially enriched after purification via FACS. This remarkable ability to identify and reconstitute rare clonotypes with defined specificities has obvious advantages in the setting of personalized medicine. Additional modifications will further enhance our ability to interrogate functional TCRs. For example, the inclusion of oligonucleotide-barcoded pMHCs will enable massively parallel screening against hundreds of recombinant pMHCs (Zhang et al., 2018),

including using a recently described approach with pseudotyped lentiviral particles (Dobson et al., 2021) that would combine effectively with renewable Jurkat-expressed TCRα:β libraries as described here. The generation of reporter libraries amenable to activation-based assays will allow the direct identification of functionally relevant TCRs, particularly for antiviral and anticancer applications. In addition, the fidelity of library screening could be enhanced via CRISPR-based homologydirected recombination, limiting the expression profile of each transformed cell to a single TCR (Vazquez-Lombardi et al., 2020). Our current approach has nonetheless addressed a major gap in functional TCRα:β profiling techniques, potentially enabling a greater understanding of adaptive immune responses and facilitating the development of more effective immunotherapeutic TCRs.

Materials and Methods

Study participants

Donor 1 enrolled in a prospective study of primary EBV infection (University of Minnesota IRB 0608 M90593). This participant developed IM at the age of 21, characterized by high fever, fatigue, body aches and headache, with a maximum illness severity of 3, as reported previously (Balfour et al., 2013). Donors 2 and 3 enrolled in an experimental antiviral drug trial (University of Minnesota IRB 0709 M16341). Donor 2 developed IM at the age of 21, characterized by fever, tender cervical lymph nodes, sore throat and fatigue, with a maximum illness severity of 5. Donor 3 also developed IM at the age of 21, characterized by fever, loss of appetite, fatigue, sore throat and headache, with a maximum illness severity of 3. Details of the trail were reported previously (Balfour et al., 2009). All donors provided written informed consent in accordance with the principles of the Declaration of Helsinki.

Sample collection and handling

Donors provided oral wash samples by gargling with 22 mL of normal saline. Suspended oral cells were pelleted and frozen in two aliquots at −80◦C. Four aliquots of supernatant were also saved and frozen at −80◦C. PBMCs were isolated from venous blood samples via density gradient centrifugation over ACCUSPIN System-Histopaque-1077 (Sigma-Aldrich, St. Louis, MO) and cryopreserved at 1 × 107 cells/mL in heat-inactivated fetal bovine serum (Thermo Fisher Scientific, Waltham, MA) containing 10% dimethyl sulfoxide (SigmaAldrich, St. Louis, MO). Cryopreserved PBMCs were thawed rapidly and diluted to 0.5 × 106 cells/mL in complete CTS OpTmizer T Cell Expansion SFM (Thermo Fisher Scientific, Waltham, MA) containing 5% CTS Immune Cell SR (Thermo Fisher Scientific, Waltham, MA), 200 IU/mL IL-2 (National Cancer Institute Preclinical Biologics Repository) and 25 µL/mL ImmunoCult Human CD3/CD28 T Cell Activator (STEMCELL Technologies, Vancouver, Canada). Cells were expanded in RPMI 1640 medium (Thermo Fisher Scientific, Waltham, MA) containing 10% heat-inactivated fetal bovine serum (Thermo Fisher Scientific, Waltham, MA), 200 IU/mL IL-2 (National Cancer Institute Preclinical Biologics Repository) and 25 µL/mL ImmunoCult Human CD3/CD28 T Cell Activator (STEMCELL Technologies, Vancouver, Canada). For the Donor 1 library, in vitro T cell expansion was used to obtain a sample that contained multiple copies of individual T cell clones for processing as two distinct Vα:Vβ sequencing replicates (Replicate 1 and Replicate 2).

Single-cell emulsification Expanded PBMCs were captured as single cells and emulsified for analyses of natively paired TCRα and TCRβ sequences using methods adapted from previous studies of antibody genes recovered from single B cells (DeKosky et al., 2015; McDaniel et al., 2016; Wang et al., 2018). Briefly, a flowfocusing device was used to encapsulate individual T cells into emulsification droplets containing lysis buffer and oligo(dT) magnetic beads (New England Biolabs, Ipswich, MA) (DeKosky et al., 2015). Magnetic beads were suspended in lysis buffer, while cells were suspended in

sterile phosphate buffered saline (PBS) at a concentration of 100,000 cells/mL. In addition to channels allowing for introduction of the bead/lysis buffer and cell/PBS mixtures, the flow-focusing device also contained a surrounding rapidly flowing oil phase comprising 4.5% (v/v) Span 80, 0.4% (v/v) Tween 80, 0.05% (v/v) Triton X-100 and 95.05% (v/v) light mineral oil (M5904, Sigma-Aldrich, St. Louis, MO). Single-cell emulsions generated by flow focusing were collected and stored on ice for 45 min. The aqueous droplets were then pooled and broken on ice using water-saturated diethyl ether (Fisher Scientific, Waltham, MA). Beads were re-emulsified in an overlap extension RT-PCR mixture using a SuperScript III RT-PCR Kit (12574018, Thermo Fisher Scientific, Waltham, MA) with the incorporation of custom designed TCR cloning primers (Supplementary Table SII) (Boria et al., 2008). Natively paired TCRα and TCRβ sequences were physically linked via an overlap in the linker between the TRBC and TRAV regions. RT-PCR was performed under the following conditions: 30 min at 55◦C, 2 min at 94◦C, four cycles comprising 30 s at 94◦C, 30 s at 50◦C and 2 min at 72◦C, four cycles comprising 30 s at 94◦C, 30 s at 55◦C and 2 min at 72◦C, and 32 cycles comprising 30 s at 94◦C, 30 s at 60◦C and 2 min at 72◦C, with a final hold for 7 min at 72◦C. RT-PCR products containing linked TCRα:β cDNA amplicons were purified using a DNA Clean & Concentrator Kit (D4033, Zymo Research, Irvine, CA).

Seminested PCR and suppression PCR

A seminested PCR was performed using a HotStart GoTaq Polymerase System (M500,1 Promega, Madison, WI). In addition to the forward and reverse primers used to amplify the paired TCRα:β templates, a set of blocking oligonucleotides complementary to the 3region of the unfused TCRα and TCRβ products was designed with several nonsense nucleotides and a phosphate group at each 3end (Turchaninova et al., 2013). These nonsense regions were intended to suppress nonnative pairing by causing a loss of homology between the elongated nonpaired TCRα and TCRβ products. The first seminested PCR was performed under the following conditions: 2 min at 95◦C and 27 cycles comprising 35 s at 95◦C, 40 s at 58◦C and 1 min at 73◦C, with a final hold for 5 min at 73◦C. The second seminested PCR was performed using a KAPA HiFi HotStart PCR Kit (7958897001, Roche, Basel, Switzerland) under the following conditions: 2 min at 95◦C and 15 cycles comprising 20 s at 98◦C, 30 s at 63◦C and 30 s at 72◦C, with a final hold for 7 min at 72◦C. PCR products were excised and purified from a 1.5% SYBR Safe Agarose Gel (Thermo Fisher Scientific, Waltham, MA).

Natively paired TCRα:β library cloning

The pLVX-EF1α-IRES-mCherry Vector (631987, Takara Bio, Mountain View, CA) was modified to enable surface expression of TCRs. After restriction enzyme digestion with BstBI and AgeI, the vector and the TCR amplicon were gel-purified and ligated using T4 DNA Ligase (M0202M, New England BioLabs Inc, Ipswich, MA), and the product was purified using a DNA Clean & Concentrator Kit (Zymo Research, Irvine, CA) and transformed via electroporation into competent MegaX DH10B T1 Electrocomp Cells (C640003, Invitrogen, Waltham, MA). Plasmids containing TCR libraries were purified using a ZymoPURE II Plasmid Maxiprep Kit (D4202, Zymo Research, Irvine, CA). The TRBC-p2A-TRAL insert was amplified using a KAPA HiFi HotStart PCR Kit (7958897001, Roche, Basel, Switzerland). TCR library plasmids and insert were digested with SpeI and MluI and ligated, transformed and purified as above. For the Donor 1 library, sequencing Replicate 1 was used for TCR library cloning and functional screening were performed using sequencing replicate 1.

HEK cell transfection and Lenti-X concentration

HEK293 adherent cells grown to a confluency of 70–90% were transfected using a Lipofectamine 3000 Reagent Kit (L3000075, Invitrogen, Waltham, MA). Transfection procedures were adapted from

the product manual. Briefly, 40 µL of Lipofectamine 3000 Reagent was diluted in 1 mL of OptiMEM Reduced Serum Medium (31985062, Gibco, Waltham, MA) and a separate master mix was prepared comprising 1 mL Opti-MEM 8 µg PSPAX (12260, Addgene, Watertown, MA), 2 µg PMD2G plasmids (12259, Addgene), 40 µL of P3000 Reagent (Thermo Fisher Scientific, Waltham, MA) and 12 µg lentiviralpLVX-EF1α-IRES-mCherry plasmid for TCR expression per T75 flask (Thermo Fisher Scientific, Waltham, MA). This master mix was added to the diluted Lipofectamine 3000 Reagent and incubated for 15 min at room temperature. The final mixture was added dropwise to the flask containing HEK293 cells and incubated for 3 days at 37◦C. Viral supernatants from transfected HEK293 cells were collected and centrifuged at 800 × g for 10 min. For transduction of J.RT3-T3.5/CD8 cells and SKW-3 cells, viral stocks were concentrated by adding supernatant at a 3:1 ratio to LentiX Concentrator (631232, Takara Bio, Mountain View, CA). Mixtures were incubated overnight at 4◦C. Samples were centrifuged at 1500 × g for 45 min at 4◦C. Pellets were resuspended in 1 mL RPMI 1640 medium and stored at −80◦C.

TCR transduction

CD8 expression was engineered into the Jurkat-derived J.RT3-T3.5 cell line, which lacks TCRβ expression (ATCC, Manassas, Virginia). A construct encoding CD8β and CD8α was cloned into a retrovirus and transduced into J.RT3-T3-5 cells to generate the J.RT3-T3.5/CD8 clone, facilitating more stable interactions between expressed TCRs and cognate pMHCs. For each transduction, 3 × 106 J.RT3-T3.5/CD8 cells in 3 mL of RPMI 1640 medium were added to a single well of a 6-well plate, followed by 1 mL of the resuspended viral pellet and polybrene at a final concentration of 8 µg/mL (TR-1003, Sigma Aldrich, St. Louis, MO). After 24 h, cells were pelleted via centrifugation at 500 × g for 8 min, resuspended in 10 mL of RPMI 1640 medium, transferred to T25 flasks and incubated for 3 days at 37◦C. Cells were washed twice with PBS and sorted for mCherry expression via FACS.

Tetramer staining of immortalized cell libraries

Fluorescent pMHC tetramers conjugated to BV421 were generated as described previously (Price et al., 2005) or purchased from The Tetramer Shop ApS (Kongens Lyngby, Denmark). Each stain incorporated 1 µg of tetramer, quantified with respect to the monomeric pMHC component, and 1 × 106 TCRα:β-J.RT3-T3.5/CD8 cells in 100 µL of PBS containing 0.05% bovine serum albumin (BSA). Cells were incubated for 40 min at 37◦C and then washed three times in FACS buffer (PBS containing 0.05% BSA and 2 mM EDTA). Avidity-based screens were performed similarly via flow cytometry, using serial dilutions of each tetramer down to a concentration of 0.0039 µg/mL. In some experiments, cells were also stained with Alexa Fluor 488 antihuman TCR α/β (306712, BioLegend, San Diego, CA).

Activation assays in SKW-3 cells

Peptide pulse experiments were performed using the APC lines C1R-A2 (Price et al., 2005) and T2-B8 (a kind gift from Scott Burrows, QIMR Berghofer) matched to the appropriate donor MHC-I. Individual TCRs were cloned and packaged as lentiviruses for J.RT3-T3.5/CD8 library generation, and SKW-3 cells (ACC53, DSMZ, Braunschweig, Germany) were seeded at 0.6 × 105 cells per monoclonal TCR in 3 mL of fresh RPMI medium per well in 6-well plates. About 400 µL of the lentivirus preparation was added to SKW-3 cells. Polybrene was added at 6 µg/mL to enhance transduction efficiency, and the plates were incubated for 24 h. Cells were centrifuged at 500 g × 5 min, resuspended in 10 mL of fresh RPMI medium, transferred into T25 flasks, and incubated for 48 h. SKW-3 cells expressing mCherry were sorted on day 3. Clones were expanded to 1 × 106 cells/mL. APCs (1 × 106 cells) were transferred into 1.5 mL centrifuge tubes, washed twice with PBS and each

SKW-3 clone (1 × 106 cells) in 6-well plates overnight. Cell activation was assessed via flow cytometry after staining for CD69 (310904, BioLegend, San Diego, CA) in conjunction with CD3 (300426, BioLegend, San Diego, CA).

Bioinformatic analysis

A previously described bioinformatic pipeline was adapted to identify natively paired TCRα:β sequences (DeKosky et al., 2015; McDaniel et al., 2016; Wang et al., 2018). Modifications were incorporated to optimize the analysis of TCR genes. Raw sequences were quality-filtered and mapped to the V, D and J genes, and CDR3 sequences were identified for each read using MiXCR v2.1.12 (ref. (Bolotin et al., 2015). Sequence data were filtered to exclude out-of-frame V-(D)-J combinations, and productive in-frame junction sequences were paired by Illumina read ID and compiled by CDR3 nucleotide and V(D)J gene identity. CDR-β3 nucleotide sequences were identified and clustered to 96% nucleotide sequence identity with terminal gaps ignored (USEARCH v5.2.32) (Edgar, 2010). We defined the set of TCRα:β clones recovered as all clusters with ≥2 reads in each data set. To determine the complete TCRα:β sequence, CDR3-α:β nucleotide sequences were used as anchors to map the germline TCRα and TCRβ genes with reference to the International ImMunoGeneTics (IMGT) Information System (Lefranc et al., 2015).

Acknowledgments

We thank David O. Schmeling for help with sample preparation and collection.

Funding

This work was generously supported by grants from the Richard M. Schulze Family Foundation; the Randy Shaver Cancer Research and Community Fund; the Matt Cwiertny Foundation; the University of Minnesota Foundation; a Wellcome Trust Senior Investigator Award [100326/Z/12/Z, to D.A.P.]; the University of Kansas Cancer Center; the US Department of Defense [W81XWH1810296] and the US National Institutes of Health [DP5OD023118, P20GM103638, P20GM103418 and R21CA230487].

Ethics Statement

Clinical trials were approved by the University of Minnesota Institutional Review Board. Informed consent with permission to use stored samples for subsequent research investigations was obtained from all donors in accordance with the principles of the Declaration of Helsinki.

Data Availability

Raw sequence data were deposited in the NCBI Sequence Read Archive (SRA) under accession number PRJNA786057.

References

Aleksic, M., Dushek, O., Zhang, H., Shenderov, E., Chen, J.L., Cerundolo, V., Coombs, D. and van der Merwe, P.A. (2010) Immunity, 32, 163–174.

Azizi, E., Carr, A.J., Plitas, G. et al. (2018) Cell, 174, 1293–1308.e36

Balfour, H.H., Odumade, O.A., Schmeling, D.O., Mullan, B.D., Ed, J.A., Knight, J.A., Vezina, H.E., Thomas, W. and Hogquist, K.A. (2013) J. Infect. Dis., 207, 80–88.

Balfour, H. et al. (2009) Bailey B.B., Gabriele C., Ahmed S.F., et al. (2021) bioRxiv. 10.1101/2020.12.31.424987.

Bentzen, A.K., Marquard, A.M., Lyngaa, R. et al. (2016) Nat. Biotechnol., 34, 1037–1045.

Bolotin, D.A., Poslavsky, S., Mitrophanov, I., Shugay, M., Mamedov, I.Z., Putintseva, E.V. and Chudakov, D.M. (2015) Nat. Methods, 12, 380–381.

Boria, I., Cotella, D., Dianzani, I., Santoro, C. and Sblattero, D. (2008) BMC Immunol., 9, 50. Campillo-Davo, D., Flumens, D. and Lion, E. (2020) Cells, 9, 1720.

Corridoni, D., Antanaviciute, A., Gupta, T. et al. (2020) Nat. Med., 26, 1480–1490.

Day, E.K., Carmichael, A.J., ten Berge, I.J.M., Waller, E.C.P., Sissons, J.G.P. and Wills, M.R. (2007) J. Immunol., 179, 3203–3213.

DeKosky, B.J., Ippolito, G.C., Deschner, R.P. et al. (2013) Nat. Biotechnol., 31, 166–169.

DeKosky, B.J., Kojima, T., Rodin, A., Charab, W., Ippolito, G.C., Ellington, A.D. and Georgiou, G. (2015) Nat. Med., 21, 86–91.

DeKosky, B.J., Lungu, O.I., Park, D. et al. (2016) Proc. Natl. Acad. Sci. USA, 113, E2636–E2645. Dobson, C.S., Reich, A.N., Gaglione, S. et al. (2021) bioRxiv. 10.1101/2021.09.18.460796.

Edgar, R.C. (2010) Bioinformatics, 26, 2460–2461.

Fahad, A.S., Timm, M.R., Madan, B. et al. (2021) Front. Immunol., 12, 615102.

Gantner, P., Pagliuzza, A., Pardons, M., Ramgopal, M., Routy, J.P., Fromentin, R. and Chomont, N. (2020) Nat. Commun., 11, 4089.

Glanville, J., Huang, H., Nau, A. et al. (2017) Nature, 547, 94–98.

Grant, E.J., Josephs, T.M., Loh, L., Clemens, E.B., Sant, S., Bharadwaj, M., Chen, W., Rossjohn, J., Gras, S. and Kedzierska, K. (2018) Nat. Commun., 9, 5427.

Grimm, J.M., Schmeling, D.O., Dunmire, S.K., Knight, J.A., Mullan, B.D., Ed, J.A., Brundage, R.C., Hogquist, K.A. and Balfour, H.H. (2016) Clin. Trans. Immunol., 5, e94.

Guo, X.J., Dash, P., Calverley, M., Tomchuck, S., Dallas, M.H. and Thomas, P.G. (2016) Mol. Ther. - Methods Clin. Dev., 3, 15054.

Harris, D.T., Wang, N., Riley, T.P., Anderson, S.D., Singh, N.K., Procko, E., Baker, B.M. and Kranz, D.M. (2016) J. Biol. Chem., 291, 24566–24578.

Hu, Z., Anandappa, A.J., Sun, J., Kim, J. et al. (2018) Blood, 132, 1911–1921.

King, C.G., Koehli, S., Hausmann, B., Schmaler, M., Zehn, D. and Palmer, E. (2012) Immunity, 37, 709–720. Koning, D., Costa, A.I., Hasrat, R. (2014) J. Immunol. Methods, 405, 199–203.

Koning, D., Costa, A.I., Hoof, I. et al.(2013) J. Immunol., 190, 931–939. Krogsgaard, M. and Davis, M.M. (2005) Nat. Immunol., 6, 239–245.

Lagerman, C.E., López Acevedo, S.N., Fahad, A.S., Hailemariam, A.T., Madan, B. and DeKosky, B.J. (2019) J. Biosci. Bioeng., 128, 226–233.

Lefranc,M.-P., Giudicelli, V., Duroux, P. et al.(2015) Nucleic Acids Res., 43, D413–D422. Linette, G.P., Stadtmauer, E.A., Maus, M.V. et al. (2013) Blood, 122, 863–871.

Linnemann, C., Heemskerk, B., Kvistborg, P. et al. (2013) Nat. Med., 19, 1534–1541.

Liu, Z., Chen, O., Wall, J.B.J., Zheng, M., Zhou, Y., Wang, L., Ruth Vaseghi, H., Qian, L. and Liu, J. (2017) Sci. Rep., 7, 2193.

Ma, K.-Y., Schonnesen, A.A., He, C. et al. (2021) Nat. Immunol., 22, 1590–1598.

Madan, B., Zhang, B., Xu, K. et al. (2021) Proc. Natl. Acad. Sci. USA, 118, e2011653118. Mateus, J., Grifoni, A., Tarke, A. et al. (2020) Science, 370, 89–94.

Mayassi, T., Ladell, K., Gudjonson, H. et al. (2019) Cell, 176, 967, e19– 981.

McDaniel, J.R., DeKosky, B.J., Tanno, H., Ellington, A.D. and Georgiou, G. (2016) Nat. Protoc., 11, 429–442.

Mendoza, J.L., Fischer, S., Gee, M.H., Lam, L.H., Brackenridge, S., Powrie, F.M., Birnbaum, M., McMichael, A.J., Garcia, K.C. and Gillespie, G.M. (2020) eLife, 9, e58128.

Miconnet, I. et al. (2011) J. Immunol., 186, 7039–7049. Minervina, A.A., Pogorelyy, M.V., Kirk, A.M. et al. (2021) 10.1101/2021.07.12.21260227.

Nesterenko, P.A., McLaughlin, J., Cheng, D. et al. (2021) Proc. Natl. Acad. Sci. USA, 118, e2021190118. Newell, E.W. and Davis, M.M. (2014) Nat. Biotechnol., 32, 149–157.

Nguyen, T.H.O. et al. (2014) J. Immunol., 192, 5039–5049. Ornatsky, O., Baranov, V.I., Bandura, D.R., Tanner, S.D. and Dick, J. (2006) J. Immunol. Methods, 308, 68–76.

Overall, S.A., Toor, J.S., Hao, S. et al. (2020) Nat. Commun., 11, 1909. Price, D.A., Brenchley, J.M., Ruff, L.E. et al. (2005) J. Exp. Med., 202, 1349–1361.

Scheper, W., Kelderman, S., Fanchi, L.F. et al. (2019) Nat. Med., 25, 89–94. Schmid, D.A., Irving, M. B., Posevitz, V. et al. (2010) J. Immunol., 184, 4936–4946.

Sewell, A.K. (2012) Nat. Rev. Immunol., 12, 669–677.

Spindler,M.J., Nelson, A.L.,Wagner, E.K. et al.(2020) Nat. Biotechnol., 38, 609–619. Starr, T.N., Greaney, A.J., Hilton, S.K. et al. (2020) Cell, 182, 1295– 1310.e20.

Strønen, E., Toebes, M., Kelderman, S. et al. (2016) Science, 352, 1337–1341.

Szabo, P.A., Levitin, H.M., Miron, M. et al. (2019) Nat. Commun., 10, 4706.

Trautmann, L., Rimbert, M., Echasserieau, K., Saulquin, X., Neveu, B., Dechanet, J., Cerundolo, V. and Bonneville, M. (2005) J. Immunol., 175, 6123–6132.

Turchaninova, M.A., Britanova, O.V., Bolotin, D.A. et al. (2013) Eur. J. Immunol., 43, 2507–2515. Vazquez-Lombardi, R. et al. (2020) BioRxiv. 10.1101/2020.06.23. 166363.

Wang, B., DeKosky, B.J., Timm, M.R. et al. (2018) Nat. Biotechnol., 36, 152–155. Yossef, R., Tran, E., Deniger, D.C. et al. (2018) JCI Insight, 3, e122467.

Zhang, S.-Q., Ma, K.Y., Schonnesen, A.A., Zhang, M., He, C., Sun, E., Williams, C.M., Jia, W. and Jiang, N. (2018) Nat. Biotechnol., 36, 1156–1159. Zhang, J.-Y., Wang, X.M., Xing, X. et al. (2020) Nat. Immunol., 21, 1107–1118.

Zhang, Z., Xiong, D., Wang, X., Liu, H. and Wang, T. (2021) Nat. Methods, 18, 92–99

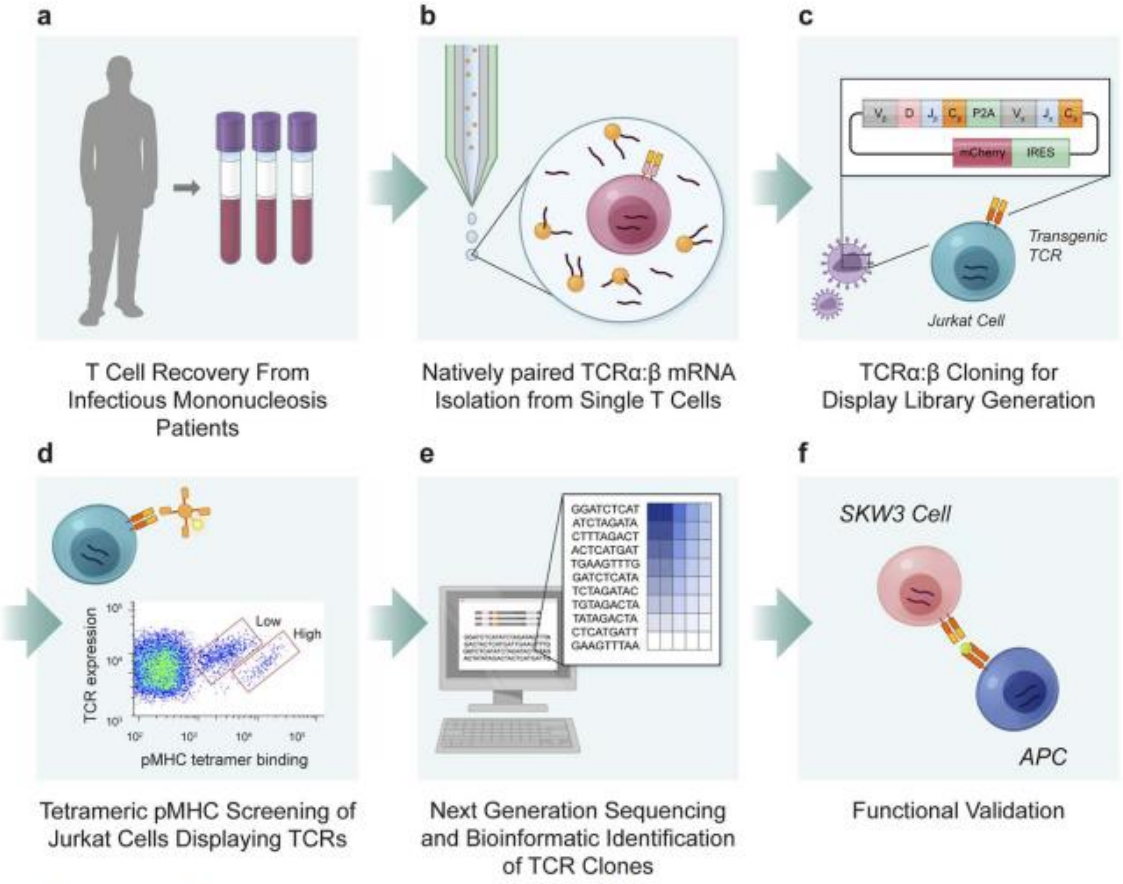

Fig. 1. High-throughput TCRα:β sequencing and functional screening of human T cell repertoires. (**a**) PBMCs were collected from patients with acute IM, and T cells were expanded briefly *in vitro*. (**b**) Single T cells were isolated into emulsion droplets for mRNA capture, and an overlap extension RT-PCR was performed to physically link TCRβ variable region (*TRBV*) and TCRα variable region (*TRAV*) sequences onto the same DNA amplicon. (**c**) TCRα:β amplicons were cloned into a lentiviral display vector containing mCherry and IRES elements, followed by a 2A translation skip motif for complete TCRα:β expression. The TCRα:β plasmids were packaged into lentiviral particles to transduce J.RT3-T3.5/CD8 cells, creating immortalized TCRα:β libraries. (**d**) TCRα:β-J.RT3-T3.5/CD8 libraries were screened via FACS for binding to a panel of pMHC tetramers corresponding to epitopes derived from EBV. (**e**) TCR genes expressed by sorted J.RT3-T3.5/CD8 cells were characterized via NGS, and TCR sequences were tracked across sort rounds to determine the relative avidity and specificity of individual TCRs. (**f**) Monoclonal TCRs were transduced into SKW-3 cells, and activation was assessed in response to pMHCs on the surface of APCs.

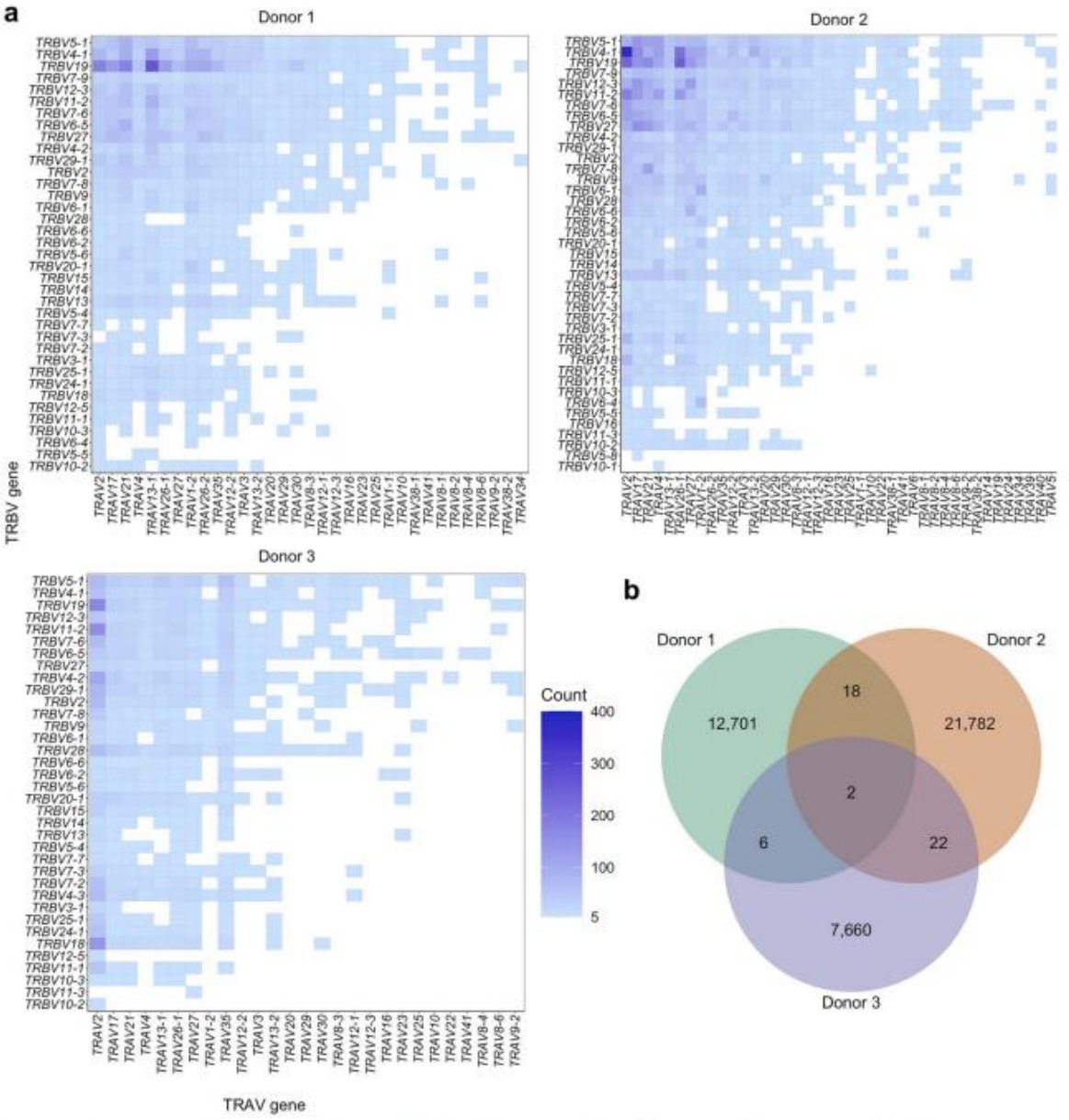

Fig. 2. Genetic analysis of TCRα:β repertoires. (**a**) Paired *TRBV*:*TRAV* gene usage recovered from three patients with acute IM. (**b**) Genetic overlap of CDR-β3 nucleotide sequences among patients with IM. Shared clonotypes with a read difference > 50-fold across samples were not included due to the potential for MiSeq index hopping during Illumina sequencing runs.

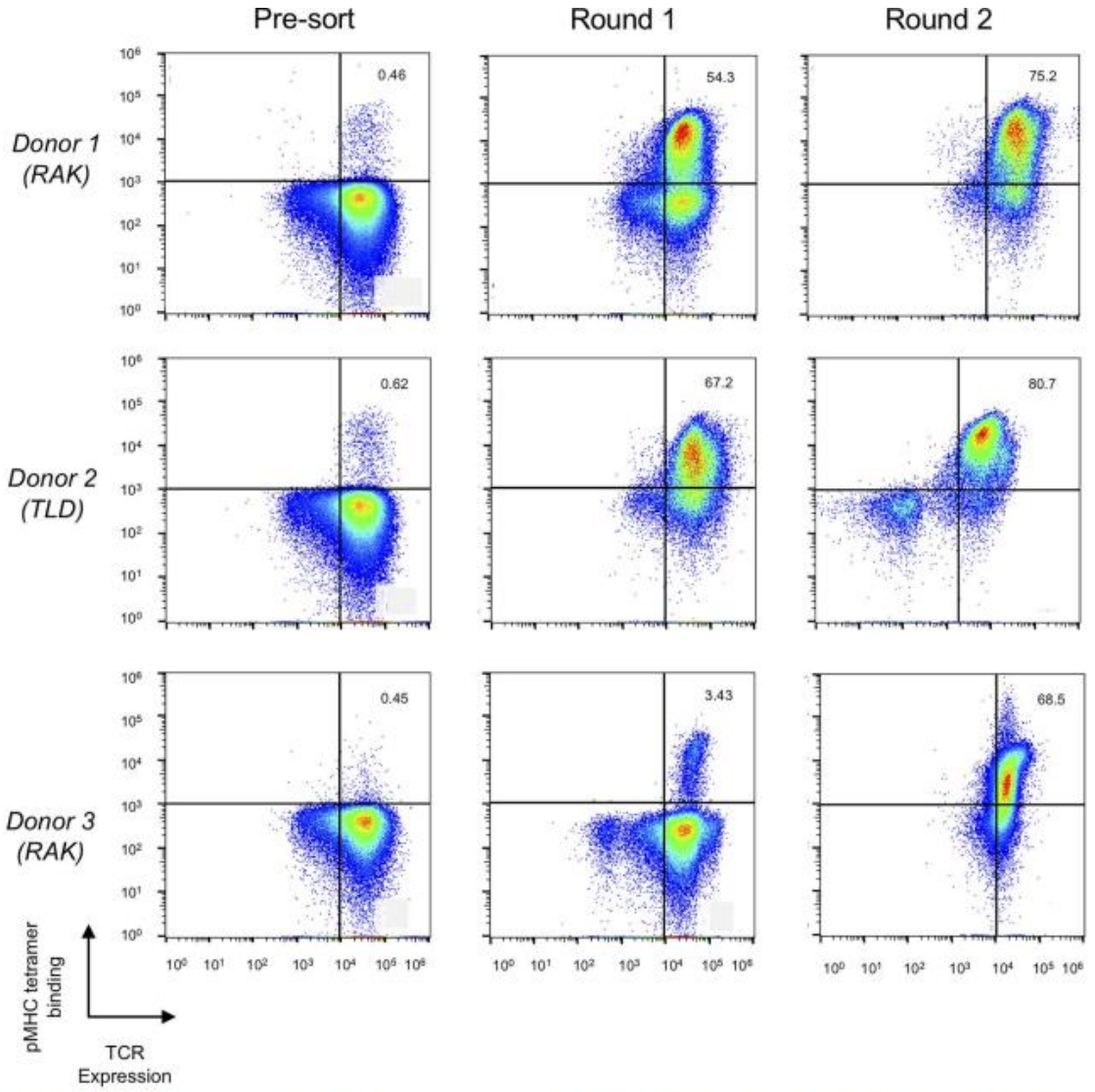

Fig. 3. Functional screening of TCRα:β-J.RT3-T3.5/CD8 libraries against pMHC tetramers. (**a**–**c**) TCRα:β-J.RT3-T3.5/CD8 libraries were enriched via sequential rounds of FACS for TCRs that bound specific pMHCs. TCRα:β-J.RT3-T3.5/CD8 libraries were stained with pMHC tetramers corresponding to epitopes derived from EBV, namely TLD/HLA-A*02:01 and RAK/HLA-B*08:01. TCR expression is shown on the *x*-axis, and tetramer binding is shown on the *y*-axis.

Table I. Genetic features of recovered TCRα:β clones

Clone no.	Donor	Target peptide	TRBV	TRBJ	TRAV	TRAJ	CDR3β	CDR3α
1	Donor 1	RAK	TRBV5–4	TRBJ1–1	TRAV35–2	TRAJ43	CASSWGT-GENTEAFF	CAGCFNDMRF
2	Donor 1	RAK	TRBV27–1	TRBJ2–2	TRAV26–1	TRAJ24	CASSPLT-GELFF	CIVRVG-GDSWGKLQF
3	Donor 1	RAK	TRBV27–1	TRBJ2–1	TRAV13–1	TRAJ50	CASSFW-DRVNEQFF	CAAMETSYD-KVIF
4	Donor 1	TLD	TRBV6–6	TRBJ1–1	TRAV26–2	TRAJ48	CASRGWRN-TEAFF	CIP-SLSNFGNEKLTF
5	Donor 1	QAK	TRBV5–1	TRAJ28	TRAV35–1	TRAJ28	CASSLETNAY-GYTF	CAGQ-TAYSGAGSYQLTF
6	Donor 1	QAK	TRBV5–1	TRBJ2–3	TRAV35–01	TRAJ28	CASSLEL-GSPDTQYF	CAGQ-PLYSGAGSYQLTF
7	Donor 1	RAK	TRBV27	TRBJ2–3	TRAV26–1	TRAJ26–1	CASSPLT-DTQYF	CIVR-VAGDSWGKLQF
8	Donor 1	RAK	TRBV5–1	TRBJ1–3	TRAV13–2	TRAJ45	CASSF-SSEGGGN-TIYF	CAEWG-WSGGGADGLTF
9	Donor 2	TLD	TRBV28–1	TRBJ1–2	TRAV30–1	TRAJ52	CASSYRTDY-GYTF	CGTINGGT-SYGKLTF
10	Donor 3	RAK	TRBV27–1	TRBJ2–3	TRAV27–2	TRAJ44	CASSTLNS-DRGADTQYF	CAGWTG-TASKLTF
11	Donor 3	RAK	TRBV12–3	TRBJ2–2	TRAV13–1	TRAJ50	CASLILGRS-DTGELFF	CAASETSYDKVI

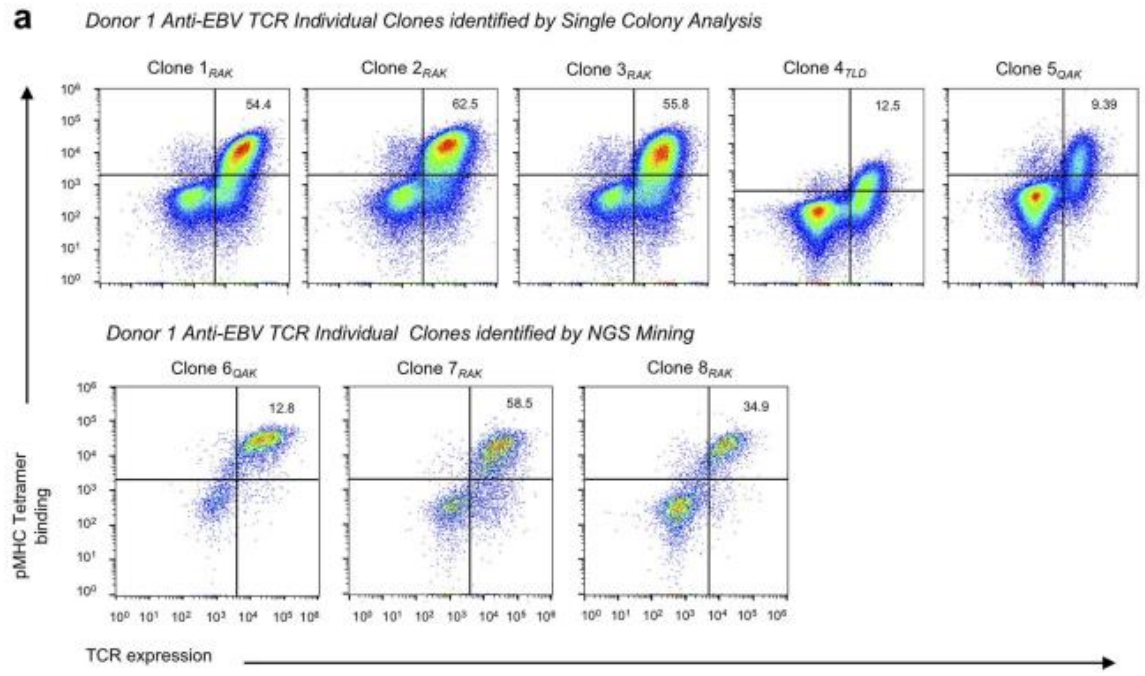

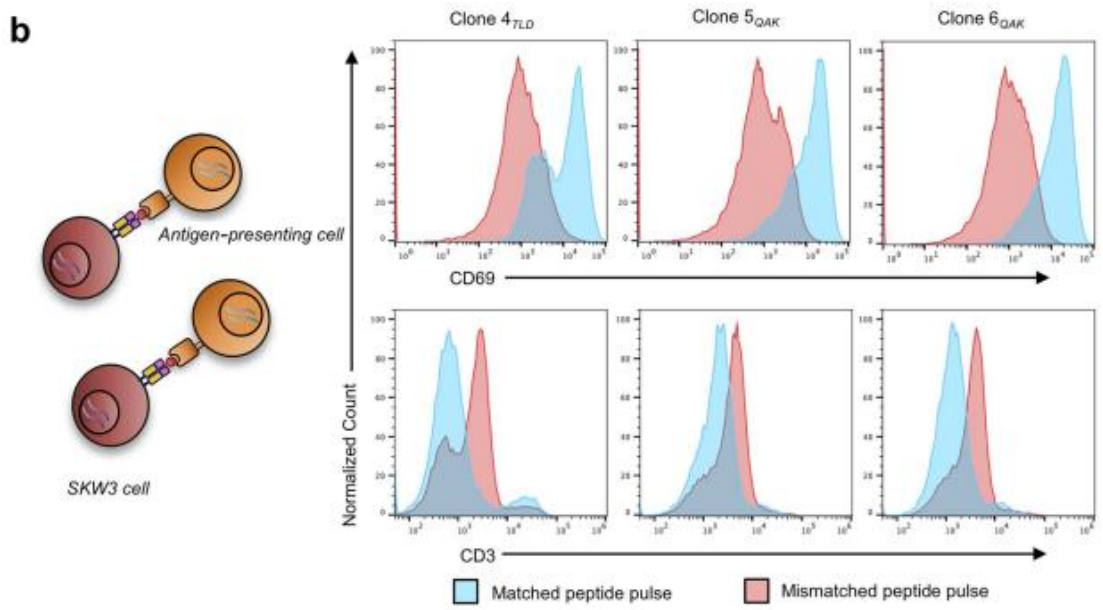

Fig. 4. Functional validation of monoclonal TCRs recovered from high-throughput screening via NGS. (**a**) TCRα:β genes were transduced into J.RT3-T3.5/CD8 cells and validated for binding against cognate pMHCs. TCR expression is shown on the *x*-axis, and pMHC binding is shown on the *y*-axis. (**b**) Monoclonal TCRα:β-SKW-3 cells were assessed for activation in response to pMHCs on the surface of APCs. CD69 or CD3 expression is shown on the *x*-axis, and normalized counts are shown on the *y*-axis.

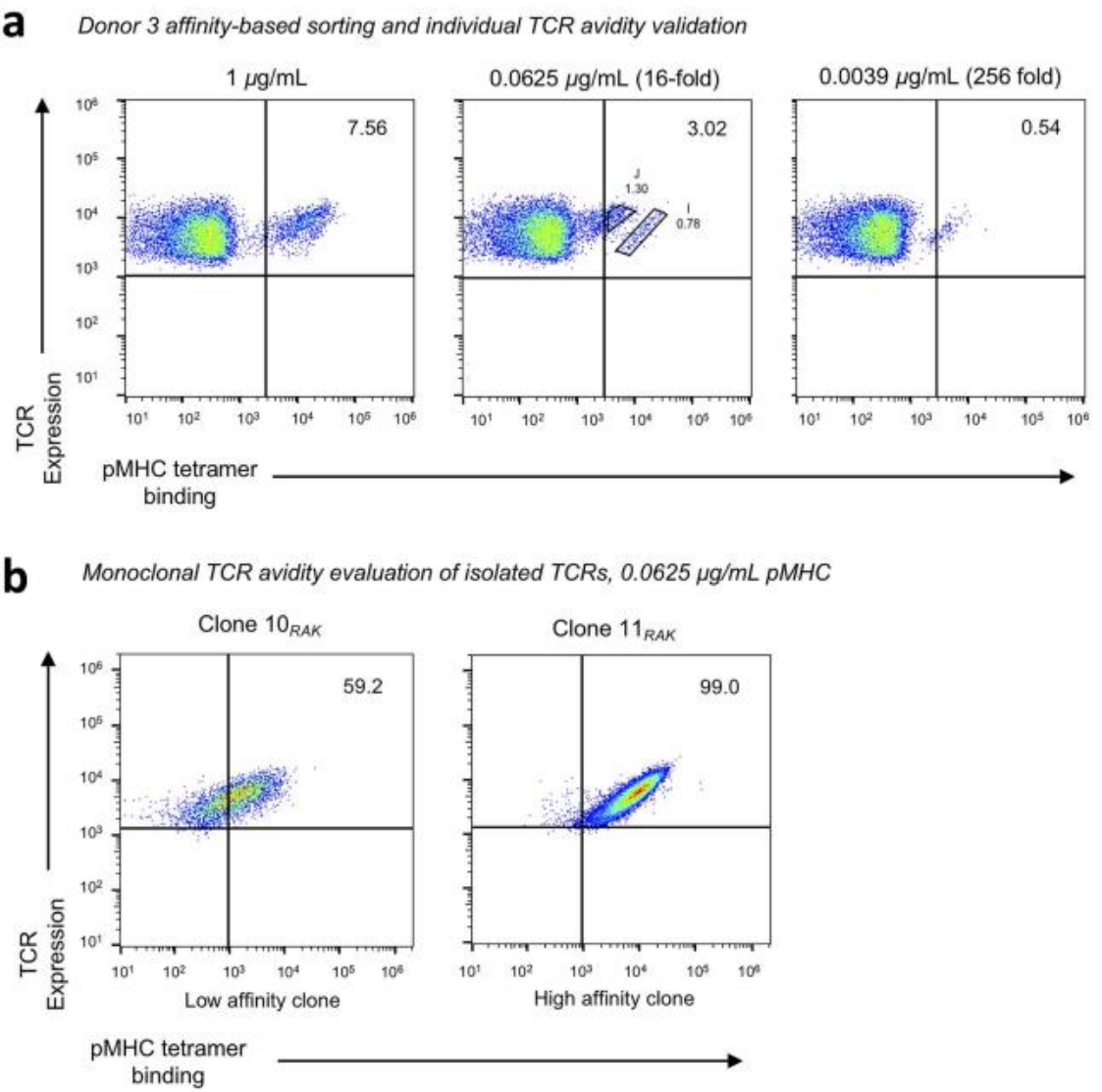

Fig. 5. Avidity-based isolation of TCRα:β-J.RT3-T3.5/CD8 cells. (**a**) TCR avidity was assessed against a gradient of pMHC tetramer concentrations, measuring TCR binding to the corresponding soluble antigens via FACS. Avidity-based sorts were performed from the Donor 3 library after 1 round of enrichment on the relevant pMHC. (**b**) Individual TCR clones identified in (a) were validated for pMHC binding at tetramer concentrations of 0.0625 μg/mL. Tetramer binding is shown on the *x*-axis, and TCR expression is shown on the *y*-axis.